Self-Assembled Epitaxial Nanocomposite BaTiO 3 –NiFe 2 O 4 Films Prepared by Polymer-Assisted Deposition

ARTICLE *in* JOURNAL OF THE AMERICAN CHEMICAL SOCIETY · DECEMBER 2007

Impact Factor: 12.11 · DOI: 10.1021/ja075764u · Source: PubMed

12 AUTHORS, INCLUDING:

Menka Jain
University of Connecticut
112 PUBLICATIONS **1,480** CITATIONS
SEE PROFILE

Thomas Mark Mccleskey
Los Alamos National Laboratory
122 PUBLICATIONS **2,130** CITATIONS
SEE PROFILE

Terry G. Holesinger
Los Alamos National Laboratory
211 PUBLICATIONS **2,968** CITATIONS
SEE PROFILE

Quanxi Jia
Los Alamos National Laboratory
564 PUBLICATIONS **10,551** CITATIONS
SEE PROFILE

J|A|C|S
COMMUNICATIONS

Published on Web 10/31/2007

Self-Assembled Epitaxial Nanocomposite $BaTiO_3$−$NiFe_2O_4$ Films Prepared by Polymer-Assisted Deposition

Hongmei Luo,* Hao Yang, Scott A. Baily, Ozan Ugurlu, Menka Jain, Marilyn E. Hawley, T. Mark McCleskey, Anthony K. Burrell, Eve Bauer, Leonardo Civale, Terry G. Holesinger, and Quanxi Jia*

Materials Physics and Applications Division, and Materials Science and Technology Division, Los Alamos National Laboratory, Los Alamos, New Mexico 87545

Received August 1, 2007; E-mail: hluo@lanl.gov; qxjia@lanl.gov

Multiferroic materials, which show simultaneous electric and magnetic ordering, have attracted considerable interest recently due to their unusual physical properties and potential device applications.[1−4] Magnetoelectric (ME) coupling between electric and magnetic order parameters has been observed in single-phase compounds, as well as composites of either horizontal multilayer heterostructures or self-assembled vertical heterostructures.[4] The single-phase compounds and multilayer composites show weak ME coupling. On the other hand, the self-assembled epitaxial nanocomposite films show much stronger ME coupling.[5] It has been demonstrated that such nanocomposites can be formed from several combinations of ferroelectric (such as $BaTiO_3$, $PbTiO_3$, and $BiFeO_3$) and ferrimagnetic (such as $CoFe_2O_4$ and $NiFe_2O_4$) materials. For example, the ME effect has been reported in $BaTiO_3$−$CoFe_2O_4$, $BiFeO_3$−$CoFe_2O_4$, and $PbTiO_3$−$NiFe_2O_4$ nanocomposites epitaxially grown on single-crystal $SrTiO_3$ substrates.[5−17] In addition, varying the degree of strain simply by choosing different orientations of the single-crystal substrate yields different phase morphologies in these epitaxial nanocomposite films. For instance, $CoFe_2O_4$ forms nanopillars heteroepitaxially embedded in a $BaTiO_3$ matrix on a (001)-oriented $SrTiO_3$ substrate. In contrast, $BiFeO_3$ forms nanopillars embedded in a $CoFe_2O_4$ matrix on a (111)-oriented $SrTiO_3$ substrate.[5−10] It has been reported that the ME coupling and the properties of such nanocomposite films strongly depend on the morphologies and elastic interaction between the ferroelectric and the ferromagnetic phases in these epitaxial films. Furthermore, pulsed laser deposition (PLD) has been almost exclusively used to grow such self-assembled epitaxial nanocomposite films. However, chemical solution deposition techniques for the growth of thin films provide advantages such as low cost, easy setup, and coating of large areas. We have recently demonstrated that polymer-assisted deposition (PAD) based on a solution approach is a very promising technique to grow epitaxial complex metal-oxide thin films.[18] In this communication, we report the growth of epitaxial $BaTiO_3$ (BTO)−$NiFe_2O_4$ (NFO) nanocomposite films on single-crystal (001)-oriented $LaAlO_3$ (LAO) substrates using the PAD technique.

The precursor solution for the growth of BTO−NFO nanocomposite films (molar ratio of BTO to NFO is 1:1) was prepared by mixing individual aqueous solutions of Ba, Ti, Ni, and Fe bound to ethylenediaminetetraacetic acid (EDTA) and polyethyleneimine (PEI) polymers (see Supporting Information for details). The precursor films were spin-coated onto LAO substrates at 2000 rpm for 30 s. Self-assembled epitaxial nanocomposite films were accomplished by annealing the films at 950 °C for 1 h. Figure 1a shows the X-ray diffraction (XRD) $\theta-2\theta$ scan for a 50 nm thick BTO−NFO thin film on a LAO substrate. Two-phase materials (BTO and NFO) with their *c*-axes normal to the substrate are clearly seen from the diffraction patterns. Figure 1b displays the ϕ scans

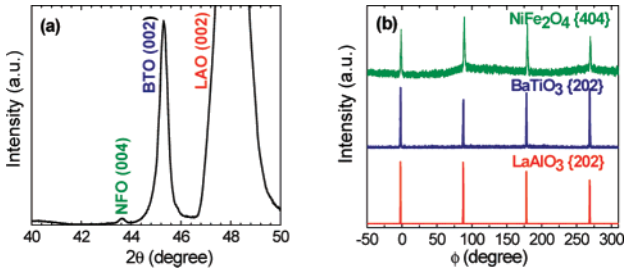

Figure 1. XRD patterns of the BTO−NFO composite film on LAO substrate: (a) $\theta-2\theta$ scan; (b) ϕ scans from (202) reflections of BTO and LAO and (404) reflection of NFO.

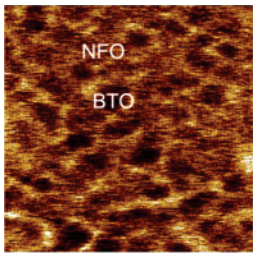

Figure 2. AFM surface potential image of the BTO−NFO composite film (1 μm × 1 μm).

on reflections of LAO {202}, BTO {202}, and NFO {404} of this composite film. The epitaxial growth of both BTO and NFO on LAO can be obviously deduced from these aligned peaks. The epitaxial relationships can be described as $(001)_{NFO}||(001)_{BTO}||(001)_{LAO}$ and $[101]_{NFO}||[101]_{BTO}||[101]_{LAO}$. Such epitaxial relationships can be understood by considering the basal plane lattice constants of BTO ($a = 0.399$ nm), NFO ($a = 0.834$ nm), and LAO ($a = 0.379$ nm). The lattice mismatch between BTO and LAO is 5.3%, but 10% between NFO and LAO (2×) lattice. Such lattice mismatches make it possible to epitaxially grow both BTO and NFO on LAO substrates. It should be noted that the epitaxial quality is quite good with an average full width at half-maximum (fwhm) value of 0.8° for BTO and 1.4° for NFO, as compared to 0.7° for the single-crystal LAO substrate.

Figure 2 shows an atomic force microscopy (AFM) surface potential image of a BTO−NFO film. The composite film clearly contains well-defined BTO (dark regions in the image) and NFO phases (light regions in the image). From the AFM analysis of the pure NFO, BTO, and the composite film, NFO shows a uniform surface morphology with a homogeneous grain size of around 40 nm. The root-mean-square (rms) surface roughness is around 4 nm. However, a rms surface roughness is 20 nm for BTO. The BTO−NFO composite film has a rms surface roughness of 13 nm, and BTO grains are dispersed in the NFO matrix. Similar to the Pb-

10.1021/ja075764u CCC: $37.00

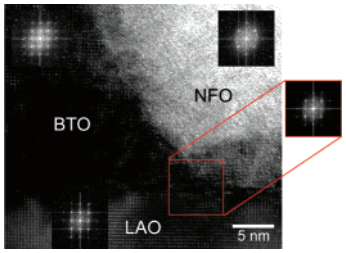

Figure 3. Cross-section HRTEM image of the BTO−NFO composite film on LAO substrate and the FFT image for the interface between phases and substrate (marked as red). Inset shows the FFT images for LAO, BTO, and NFO.

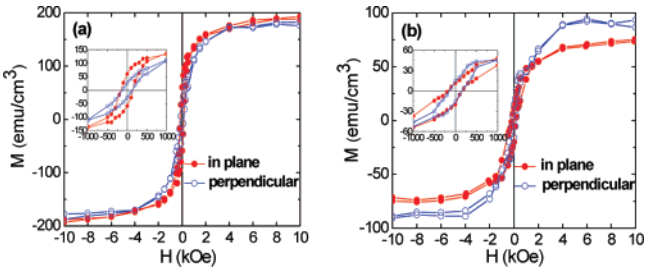

Figure 4. Magnetization versus magnetic field ($M-H$) hysteresis loops with magnetic field parallel and perpendicular to the substrate surface at 300 K for pure NFO film (a) and BTO−NFO composite film (b), respectively.

$(Zr_{0.52}Ti_{0.48})O_3$−NFO composite grown by PLD,[16] the NFO phase exists as nanoparticles instead of nanopillars in BTO−$CoFe_2O_4$ or $BiFeO_3$−$CoFe_2O_4$ composites.[5−10] However, the NFO phase is the matrix in our PAD nanocomposite films. Both the thermodynamic equilibrium and the kinetic diffusion during the process can control the growth of a self-organized epitaxial nanocomposite.[6] It has been reported that the substrate orientations can determine the morphology of the nanocomposite prepared by PLD due to the surface energy anisotropy.[10] However, the nucleation and growth, which are unique for chemical solution deposition, may play a critical role in determining the surface morphology of BTO−NFO in our case.

Figure 3 shows a cross-section high-resolution transmission electron microscopy (HRTEM) image of a BTO−NFO film on LAO substrate and the Fast Fourier Transform (FFT) images of BTO, NFO LAO, and the interface between the two phases and substrate (marked in red). The d spacing measured from the corresponding FFT matches the lattice parameters of BTO, NFO, and LAO. The cross-section HRTEM and the interface FFT images show the clear epitaxial relationship between the two phases and the substrate. The sharp interface between the nanocomposite film and the substrate can be seen as well. The spectral images (Figure S1) also show the BTO and NFO phases.

Our BTO−NFO composite films exhibit both ferroelectric and ferrimagnetic properties. The polarization versus electric field ($P-E$) hysteresis characteristics of the Pt/BTO−NFO/SRO capacitor (Figure S2) indicate the ferroelectric nature of the composite film. The leakage current density (J) versus electric field (E) characteristic (Figure S3) shows that the film has a leakage current density of $\sim 10^{-4}$ A/cm^2 even at a magnetic field of 10^6 V/cm. Figure 4 shows the magnetization versus magnetic field ($M-H$) hysteresis loops with the magnetic field parallel and perpendicular to the substrate surface at 300 K for a pure NFO film (Figure 4a) and a BTO−NFO composite film (Figure 4b), respectively. The similar characteristics along in-plane and out-of-plane directions imply small magnetic anisotropy in both the composite BTO−NFO and pure NFO films except there is a slightly higher magnetization for the out-of-plane for the composite film. The saturation magnetization value for the composite film is about 80−90 emu/cm^3, almost half of the pure NFO film, consistent with the molar fraction of NFO in the composite film. The composite film has a coercivity of 150 Oe, about 10 Oe higher than the pure NFO film.

In summary, we demonstrate that a cost-effective chemical solution technique can be used to grow self-assembled epitaxial BTO−NFO nanocomposite films. Ferroelectric BTO is embedded in the ferrimagnetic spinel NFO matrix. The composite shows both ferroelectric and ferromagnetic properties.

Acknowledgment. This work was supported by the LDRD Project at Los Alamos National Laboratory under the U.S. Department of Energy (DOE) and by the DOE Solid State Lighting Program managed by DOE EE-RE.

Supporting Information Available: Complete ref 5 and solution, film preparation, and characterization of the BTO−NFO nanocomposite. This material is available free of charge via the Internet at http://pubs.acs.org.

References

(1) Spaldin, N. A.; Fiebig, M. *Science* **2005**, *309*, 391.
(2) Eerenstein, W.; Mathur, N. D.; Scott, J. F. *Nature* **2006**, *442*, 759.
(3) Cheong, S.-W.; Mostovoy, M. *Nat. Mater.* **2007**, *6*, 13.
(4) Ramesh, R.; Spaldin, N. A. *Nat. Mater.* **2007**, *6*, 21.
(5) Zheng, H.; et al. *Science* **2004**, *303*, 661.
(6) Zheng, H.; Wang, J.; Mohaddes-Ardabili, L.; Wuttig, M.; Salamanca-Riba, L.; Schlom, D. G.; Ramesh, R. *Appl. Phys. Lett.* **2004**, *85*, 2035.
(7) Chang, K.-S.; Aronova, M. A.; Lin, C.-L.; Murakami, M.; Yu, M.-H.; Hattrick-Simpers, J.; Famodu, O. O.; Lee, S. Y.; Ramesh, R.; Wuttig, M.; Takeuchi, I.; Gao, C.; Bendersky, L. A. *Appl. Phys. Lett.* **2004**, *84*, 3091.
(8) Zavaliche, F.; Zheng, H.; Mohaddes-Ardabili, L.; Yang, S. Y.; Zhan, Q.; Shafer, P.; Reilly, E.; Chopdekar, R.; Jia, Y.; Wright, P.; Schlom, D. G.; Suzuki, Y.; Ramesh, R. *Nano Lett.* **2005**, *5*, 1793.
(9) Zheng, H.; Straub, F.; Zhan, Q.; Yang, P.-L.; Hsieh, W.-K.; Zavaliche, F.; Chu, Y.-H.; Dahmen, U.; Ramesh, R. *Adv. Mater.* **2006**, *18*, 2747.
(10) Zheng, H.; Zhan, Q.; Zavaliche, F.; Sherburne, M.; Straub, F.; Cruz, M. P.; Chen, L.-Q.; Dahmen, U.; Ramesh, R. *Nano Lett.* **2006**, *6*, 1401.
(11) Zhan, Q.; Yu, R.; Crane, S. P.; Zheng, H.; Kisielowski, C.; Ramesh, R. *Appl. Phys. Lett.* **2006**, *89*, 172902.
(12) Zheng, H.; Kreisel, J.; Chu, Y.-H.; Ramesh, R.; Salamanca-Riba, L. *Appl. Phys. Lett.* **2007**, *90*, 113113.
(13) Li, J. H.; Levin, I.; Slutsker, J.; Provenzano, V.; Schenck, P. K.; Ramesh, R.; Ouyang, J.; Roytburd, A. L. *Appl. Phys. Lett.* **2005**, *87*, 072909.
(14) Levin, I.; Li, J. H.; Slutsker, J.; Roytburd, A. L. *Adv. Mater.* **2006**, *18*, 2044.
(15) Ortega, N.; Bhattacharya, P.; Katiyar, R. S.; Dutta, P.; Manivannan, A.; Seehra, M. S.; Takeuchi, I.; Majumder, S. B. *J. Appl. Phys.* **2006**, *100*, 126105.
(16) Ryu, H.; Murugavel, P.; Lee, J. H.; Chae, S. C.; Noh, T. W.; Oh, Y. S.; Kim, H. J.; Kim, K. H.; Jang, J. H.; Kim, M.; Bae, C.; Park, J.-G. *Appl. Phys. Lett.* **2006**, *89*, 102907.
(17) Slutsker, J.; Levin, I.; Li, J.; Artemev, A.; Roytburd, A. L. *Phys. Rev. B* **2006**, *73*, 184127.
(18) Jia, Q. X.; McCleskey, T. M.; Burrell, A. K.; Lin, Y.; Collis, G. E.; Wang, H.; Li, A. D. Q.; Foltyn, S. R. *Nat. Mater.* **2004**, *3*, 529.

JA075764U